



MAGNETIC FIELD EVALUATION AROUND 400 KV UNDERGROUND POWER CABLE UNDER HARMONICS EFFECTS

Houari BOUDJELLA ^{1,*} , Ahmed N. E. I AYAD ¹ , Tahar ROUIBAH ¹, Benyekhlef LAROUCI ¹ , Thamer A. H ALGHAMDI ² , Ahmed ALTHOBAITI ³ , Sherif S. M. GHONEIM ³ , Abdelkader Si TAYEB ⁴

¹ Department of Electrical Engineering, Kasdi Merbah University, Ghardaia Road, P.O. Box 511, Ouargla 30000 DZ, Algeria

² School of Engineering, Cardiff University, Cardiff, UK

³ Department of Electrical Engineering, College of Engineering, Taif University, P.O. Box 11099, Taif 21944, Saudi Arabia

⁴ Applied Research Unit for Renewable Energies "URAER Ghardaia", Renewable Energy Development Center (CDER), Ghardaia 47133, Algeria

E-mail : boudjella.houari@univ-ouargla.dz

Abstract

Power lines or underground power cables generate electromagnetic interaction with other objects near to them. This study evaluates the magnetic field emitted by underground extra high voltage cables. The presented work aims to show a numerical simulation of the magnetic field of a buried 400 kV underground power line, which is used as a novel prototype in several countries at a short distance. The underground power cable study, in the presence of the current harmonics at different positions, with time variation by finite element resolution, using Comsol Multiphysics with Matlab software in two dimensions. The simulation results illustrate the magnetic flux density variation-in terms of amplitude and distribution as a function of different actual harmonics rates. The underground cable performance and magnetic field have affected by the harmonics effects. The maximum magnetic induction levels generated by significant harmonics are superior to the limits recommended by the international standard norms. In this paper, shielding has been used as an appropriate remedy to attenuate the magnetic field.

Keywords: electric power cables, magnetic field, harmonics, shielding, 400 kV underground power system.

1. INTRODUCTION

In recent years, the use of very high voltage (VHV) and extra high voltage (EHV) cables in electric networks have been increasing due to the developments and extensions of underground and submarine power cable systems in populated areas driven by environmental constraints [1]–[3]. Although underground cables transmit power through urban areas, the hidden nature of cables protect area from visually pollute [4]–[6].

The electromagnetic interferences (EMI) are produced by two different kinds: inductive and capacitive coupling between the three-phase underground power lines and the nearby objects or pipes lines [4]. The study and the simulation of the electromagnetic fields in several underground power cables, are essential to show the electromagnetic interactions and interferences produced around and near them [5], [6].

Many researchers have been worked on the development of models for computing magnetic

fields (MF) emitted by overhead, underground or subsea lines of VHV, HV and MV, on the other hand, few studies on EHV cables and lines with time variation (using analytical and numerical models in stationary studies) [3], [7], [8]. Due to the high demand for electrical power and the significant expansion of overhead transmission lines (OHLs) and underground power cables (UPCs), there is greater exposure to the magnetic fields (MF) generated by them. However, the MFs has led to an increased demand for ensuring the safety of people exposed to human electrical sensitivity as well as human immunodeficiency [9]. This requires to a large extent the design and modernization of measures to mitigate the interference coming from the extremely low frequency (ELF) magnetic fields (50/60Hz), which in turn affects the performance of electrical and electronic devices and reduces their efficiency as well [10].

As is known, exposure to magnetic flux should be limited between 3 and 100 (μ T) [10], [11]. As a result, maintaining its value within acceptable limits

is critical in the design and development of magnetic flux mitigation measures. Several MF shielding technologies have been proposed and improved in the last twenty years, such as the use of conductor arrangement, metallic plates, raceways, horizontal, U-reverse magnetic, and H-shaped shields, passive and active loops techniques, and passive shields [12].

Various research works have been conducted on the MF produced by UPCs. However, some of them have used analytical approaches, while others are based on numerical and experimental techniques [13]–[15]. In [15], the MF generated by a practical in-service underground pipe-type cable was calculated using a computational model finite element method (FEM) combined with the semi-analytical boundary element method (BEM) is proposed in [16] to reevaluate MF due to UPCs. ELF-MF was caused by a three-phase UPC and its dosimetry analysis for a human model was treated using both analytical and FEM computations in [17]. A detailed review of optimization methods used for MF mitigation in OHLs and UPCs can be found in [9]. Authors in [18], suggested an optimized grid composed of a set of n_m conductors, parallel to the power cables, to mitigate the MF originated by UPC. Mitigation of magnetic flux density (MFD) of UPC and its conductor term temperature-based FEM is discussed in reference [19]. MF shielding of UPC by an H-shaped shield is adopted in [20]. A 4-mm reverse U-shaped copper material is proposed in [17] to mitigate the MF caused by UPC.

This paper focuses on the electromagnetic simulation by FEM carried out on a new 400 kV UPCs system. This kind of cable has been used as a prototype in several countries at a short distance. Several parameters affecting the magnetic induction emission can be studied, such as distance, power, and soil nature. In this work, we choose the presence of harmonics and time depending on the parameters' influence. The simulation model used in this study consists of three single-phases EHV electric underground power cable systems. The magneto dynamic model of Comsol Multiphysics is used with MATLAB Simulink environment. The underground line has been simulated in two scenarios; (i) steady states, and (ii) withering the presence of current harmonics in three cables of the transmission line.

This work aims also to calculate the magnetic distribution and detailed evaluation of MF emitted at the ground surface by high voltage buried cables in urban areas (one meter above ground) and show the effect of the harmonic on magnetic field intensities. Finally, the simulation results will be compared with tolerable emission levels according to IEEE, ICNIRP and other European standards limits [10]. In addition, the shielding efficiency for the MF attenuation (aluminium plate), is simulated to reduce the ground-level magnitude. It is important to specify if this study targets electromagnetic compatibility (EMC) issues or health/ecology issues, as different field levels may apply.

2. GEOMETRY AND CHARACTERISTIC OF EHV CABLE

A cross-section area of the cable used in this study is shown in Fig. 1.

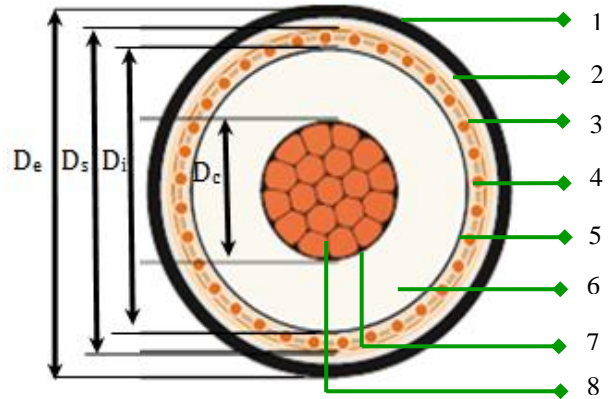


Fig. 1. 400 kV HV power cable cross-section

The characteristics of the individual cable layers are given in Table 1 [21].

Table 1. Description of 400 kV power cable layout materials

| Layer No. | Description |
|-----------|----------------------------|
| 1 | Polyethylene sheath |
| 2 | Aluminium tape |
| 3 | Copper wire screen |
| 4 | Watertight design |
| 5 | Insulation screening |
| 6 | XLPE insulation |
| 7 | Conductor screening |
| 8 | Aluminium/copper conductor |

The cross-section dimensions of the 400 kV power cable are given in Table 2.

Table 2. Dimensions of 400 kV underground power cable

| Cable dimension | Symbol | Values |
|---|----------------|--------|
| Cross-section of the conductor (mm ²) | S | 3000 |
| Diameter of the conductor (mm) | D _c | 68.4 |
| The outer diameter of the cable (mm) | D _e | 148 |
| Diameter over screen (mm) | D _s | 134.8 |
| Diameter over insulation (mm) | D _i | 127.6 |

Three-phase lines composed of three such single-phase cables buried in depth (H) and laid in a flat configuration in two areas: air and soil, as shown in Fig. 2. This configuration is chosen because it gives the worst-case scenario for the MF emission in ground level [7], [22].

The 400 kV extra high voltage power cable characteristics are shown in Table 3 [21]. An underground cable mainly comprises a conductor, insulation around the conductor, screen, and concentric wires. The AC underground XLPE cables (400 kV, 3000 mm²) copper conductor the

overcurrent increase above 1.8 kA; maximum power 1250 MW [22].

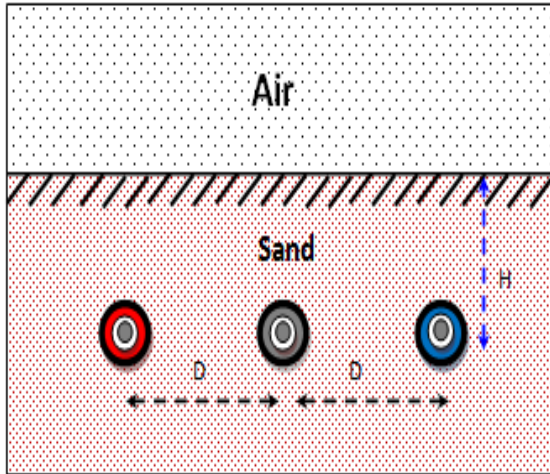


Fig. 2. Three-phase underground transmission cable at a depth of H below ground level

Table 3. 400 kV HV underground power cable characteristics

| Cable parameter | Value | Unit |
|-----------------------|-------|------|
| Voltage | 400 | kV |
| Current | 1.8 | kA |
| Depth H | 1600 | mm |
| Cable separation D | 350 | mm |
| Short circuit current | 20 | kA |

3. MAGNETIC FIELD MODEL OF EHV CABLE

Electromagnetic phenomena governed by Maxwell's equations converted in a magnetic mode in the steady-state [23]–[25]. The electromagnetic equations are given as follows:

$$\begin{cases} \text{rot } H = J' \\ D = \epsilon E \\ J' = (\sigma + j\omega\epsilon) E \\ B = \text{rot } (A) \end{cases} \quad (1)$$

Where:

E (V/m) and H (A/m) are the electric and magnetic fields respectively generated by UPC, B (T) is the magnetic flux density; A (Vs/m) denotes the magnetic vector potential; J (A/m²) presents the vector of the current density; D denotes the electric induction; ϵ stands of the permittivity, and σ (S/m) is the conductivity.

Applying the two laws of Gauss and Maxwell Ampere, it results the following equation:

$$\text{rot } H = \text{rot } (\mu^{-1}B) \quad (2)$$

Where:

μ stands of the permeability.

Substituting the expression of magnetic flux density B in the Maxwell-Faraday equation of electromagnetic induction ($\text{rot}E = -j\omega B$), we obtain:

$$\text{rot } E = -j\omega(\text{rot } A) = \text{rot}(-j\omega A) \quad (3)$$

The combination of (1), (2), and (3) gives:

$$\text{rot } (\mu^{-1}\text{rot } A) = (\sigma + j\omega\epsilon) (-j\omega A) \quad (4)$$

After substitution, the formula of the final partial differential equation for the inductive effect for the following variable magnetic vector potential A in magneto-dynamic is shown as follow:

$$-\omega^2\epsilon A + j\omega\sigma A + \text{rot } (\mu^{-1}\text{rot } A) = J_s \quad (5)$$

The interface of MFs in the software uses (5) to determine the magnetic vector potential A value. Consequently, the values of all fields are derived from it (the magnetic field H and the magnetic flux density B).

Equation (5), can be written with the following equation :

$$\sigma \frac{\partial \vec{A}}{\partial t} + \text{rot } \frac{1}{\mu} \text{rot } \vec{A} = \vec{J}_s \quad (6)$$

The electric current input of the three phases is as follows [23]–[25]:

$$\begin{cases} I_a = I \cos(\omega t) \\ I_b = I \cos\left(\omega t - \frac{2\pi}{3}\right) \\ I_c = I \cos\left(\omega t + \frac{2\pi}{3}\right) \end{cases} \quad (7)$$

In order to solve the proposed mathematical problem, we use the COMSOL 4.3b Multiphysics software based on numerical finite element method (FEM), to find approximate solutions of partial differential equations of magnetic domain.

The properties of 400 kV XLPE cable materials are shown in Table 4 [23].

Table 4. Materials properties of underground extra high voltage cable

| Cable parameter | (σ) Sm ⁻¹ | (μ) | (ϵ) |
|----------------------------------|-------------------------------|-----------|----------------|
| Air | 10 ⁻¹⁴ | 1 | 1 |
| Sandy soil | 1 | 2.5 | 28 |
| Polyethylene | 10 ⁻¹⁸ | 1 | 2.25 |
| Polypropylene | 10 ⁻¹⁸ | 1 | 2.36 |
| Semi-conductive compound | 2 | 1 | 2.25 |
| Cross-linked Polyethylene (XLPE) | 10 ⁻¹⁸ | 1 | 2.5 |
| High strength alloy steel | 4.032 10 ⁶ | 1 | 1 |
| Copper | 5.096 10 ⁷ | 1 | 1 |

3.1. Finite Element Method (FEM)

The FEM analysis of any electromagnetic problem can be approximate in four steps

- Step 1: Discretization and decomposition of the model space into elements,
- Step 2: Derivation of governing equations,
- Step 3: assembly the elements in the solution space,
- Step 4: resolution and solve of all obtained equations.

The distribution of the magnetic induction B is obtained from the magnetic vector potential A .

$$B = \text{rot } (A) \quad (8)$$

In FEM, the space of the proposed each subdomain is discretized into (m) small triangular elements, formed by grid with (n) nodes. Thus, the

vector potential A at any point of different element is approximate by the shape functions N [26].

$$A(x, y) = \sum_{k=1}^m A_k \cdot N_k(x, y) \quad (9)$$

Where:

$$k = i, j, 1$$

The terms N_k is expressed as :

$$N_k = \frac{a_k + b_k \times x + c_k \times y}{2\Delta_e} \quad (10)$$

Where:

Δ_e represent the area of the triangular element, A_k is the potential at the k^{th} node.

The solution of the magnetic problem is obtain by implementation of magneto-dynamic model given by equation (6) in each subdomain. Substituting the curl of the weighting function, we take the time harmonic form of the diffusion equation we obtain [27]:

$$\iint_{\Omega} v \left(\frac{\delta A}{\delta x} \frac{\delta N}{\delta x} + \frac{\delta A}{\delta y} \frac{\delta N}{\delta y} \right) dx dy + \iint_{\Omega} (j\omega\sigma AN) dx dy = \iint_{\Omega} (J \cdot N) dx dy \quad (11)$$

Where:

$v = \frac{1}{\mu}$, represent the reluctivity.

Depending on the solution of calculated magnetic vector potential A in all nodal points, the determination of the magnetic induction B is according to equations (8) and (9). Finally, the magnetic induction equations in two-dimensional magnetics problems (2D: x, y-axis), can be written by:

$$\begin{cases} B_{xe} = \sum_{k=i,j,m} \frac{c_k}{2\Delta_e} A_k \\ B_{ye} = -\sum_{k=i,j,m} \frac{b_k}{2\Delta_e} A_k \end{cases} \quad (12)$$

Finally, from equation (12), we can calculate the total magnetic induction amplitude as below:

$$|B_T| = \sqrt{|B_{xe}|^2 + |B_{ye}|^2} \quad (13)$$

The COMSOL Multiphysics software uses the FEM to help model and simulate electromagnetic fields in several applications, (i.e. engine, cable, coil, power lines), and solve linear and nonlinear equations and complex models. Many steps characterize the software simulation [23]:

- Geometry generation model;
- The material declaration of each subdomain;
- Physics model and equations (interface conditions, the electrical and physical properties);
- Generating mesh;
- Study (stationery, frequency, temporal);
- Solve and computation;
- Plot and results visualization.

4. RESULTS AND DISCUSSION

The magnetic simulation will be studied numerically using the FEM with the COMSOL Multiphysics software [24]–[25], [28]. In this part, the underground cables is simulated in several states (steady, transient in the first single-phase, and with the presence of harmonics in a conductor). The simulation results of the conductor cross-section of copper show a significant concentration of current and Magnetic flux density in the conductor of the first single-phase see Fig. 3. As shown in Fig. 4(a), the suggested model of the 400 kV UPC, is divided into two areas: the upper is the air, and the lower is the earth. This illustration shows the arrangement and meshes of three separate cables information (Fig. 4(b)).

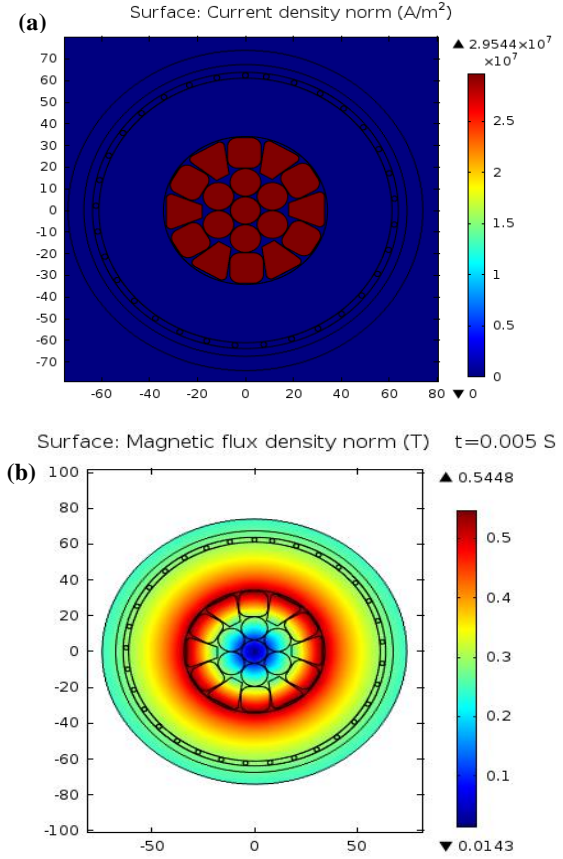


Fig. 3. Electromagnetic underground power cable characteristics, (a) Electric current density; (b) Magnetic flux density around the conductor

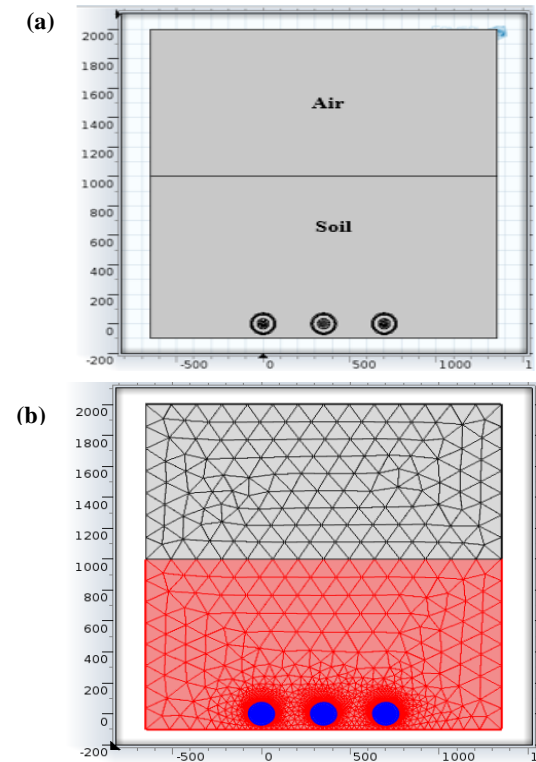


Fig. 4. Simulation model of UPC system, (a) Configuration of the simulation model, (b) Meshing of the three-phase cable system

Fig. 5(a) and Fig. 5(b) show respectively, the magnetic vector potential and the magnetic field lines near the underground power cable system of EHV.

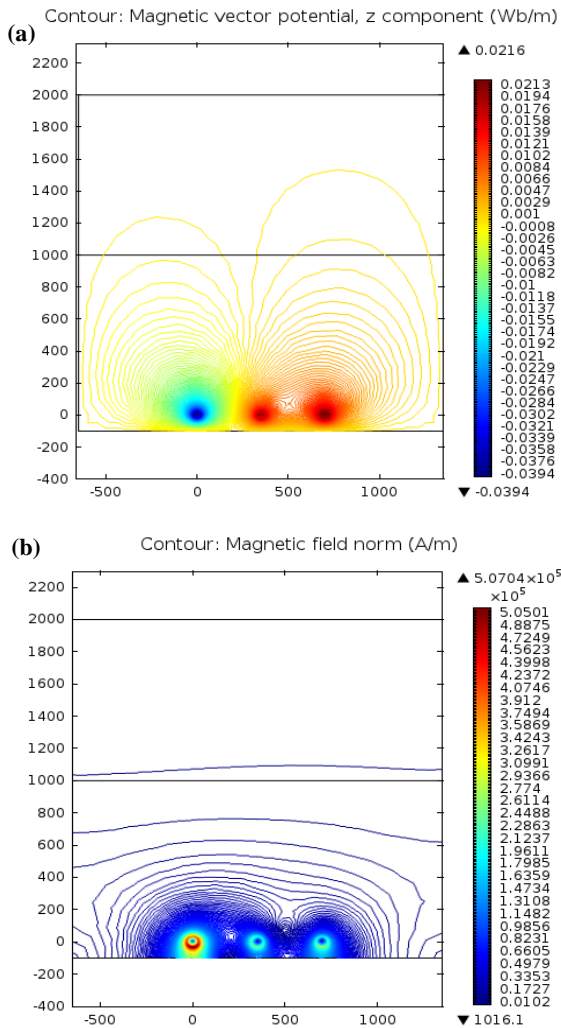


Fig. 5. Magnetic distribution of EHV cable systems, (a) Magnetic vector potential distribution; (b) Magnetic field around the underground cable

Distribution is critical in EHV cables due to the incredible intensity of the current in the three cables of each line. Overall, above the ground-level magnetic field from cables fall much more rapidly with distance, but higher in small spaces from the cable. There are always electromagnetic interferences (EMI) between the electric cables and devices as both the inductive and capacitive phenomena.

4.1. Instantaneous simulation of the UPCs

Three underground cables supplied by three sine currents waves in steady-state. The simulation result shows the horizontal and vertical distribution (along the two axes x and y) of the magnetic flux density at several levels concerning the ground (ground level and near the cables) above the UPCs.

Fig. 6 shows the calculation of the magnetic induction in $Y=0$ (ground level) as a function of time and distance. Moving away from the three electric cables, the magnetic flux density decrease and will be less important in both directions.

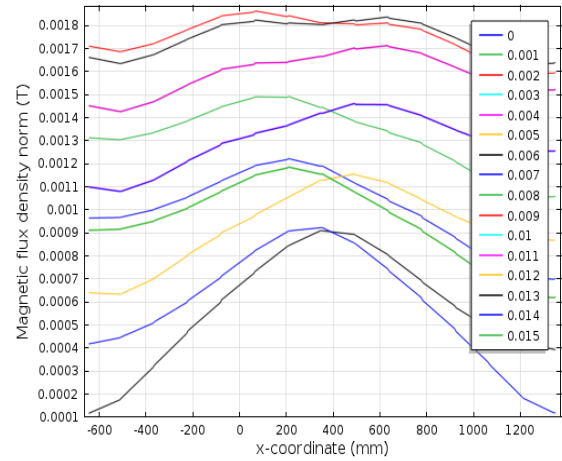


Fig. 6. Variation of magnetic flux density in $Y=0$ as a function of time and distance of three cables underground

Fig. 7 shows the calculation of the magnetic flux density near the three cables as a function of distance and time depending. The magnetic flux density is significant besides the electric cables, in the two directions. There are several curves because the system is sinusoidal and will depend on time variation (time variation represented by a different color).

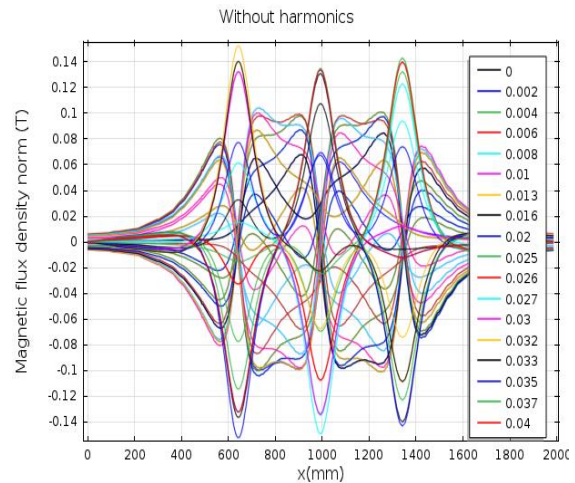


Fig. 7. Magnetic flux density (B_x, B_y) as a function of time near the three cables

4.2. Presence of the harmonics current

The presence of harmonics current in the conductor results in a sizeable deformation of the total current, which will affect the electromagnetic field. The MFD with harmonics increases and decreases as a function of THD rate and harmonics rang [29]. The EHV-UPCs connected in power grid affected by power quality and harmonic flow [29], [30].

Table 5. Exposure limits for the both general public and occupational (workers) for electromagnetic fields at 50/60 Hz.

| Norm Scope | Council EU 1999 | | | ICNIRP 2010 | | | IEEE 2019 | | |
|----------------|-----------------|-------------|-----------------|-------------|-------------|-----------------|-------------|-------------|-----------------|
| | E (KV/m) | H (KA/m) | B (μ T) | E (KV/m) | H (KA/m) | B (μ T) | E (KV/m) | H (KA/m) | B (μ T) |
| General public | 5 | - | 100 | 4.2 | 0.16 | 200 | 5 | 0.719 | 904 |
| Occupational | 20 | - | 6000 | 8.3 | 0.8 | 1000 | 20 | 2.16 | 2710 |

Many recommendations were adopted to protect the citizens against electromagnetic fields [31], [32]. The lower exposure limits provided for low power frequencies fields according to Council EU (1999) [11], ICNIRP (2010) [33], and IEEE (2019) [34], are reported in Table 5.

Many studies and experience grid shows that the most significant harmonics rang are Ih3 (canceled by using star coupling), 5th, 7th, 11th, and 13th harmonics, and the least significant harmonics are the pair harmonics and multiple. The dominant harmonics are critical in 400 kV underground lines generated in practice by converter stations [29-30], [35]. To illustrate the influence of harmonics in underground electric cables, four cases with different percentages of harmonics without the fundamental current has been studied. The supposed values of four THD are respectively 2.8 %, 3.6 %, 4 %, and 4.7 % with harmonics rang Ih5, Ih7, Ih11, and Ih13. We choose several levels and order of harmonics respecting the experimental measurements [35], as represented in Fig. 8.

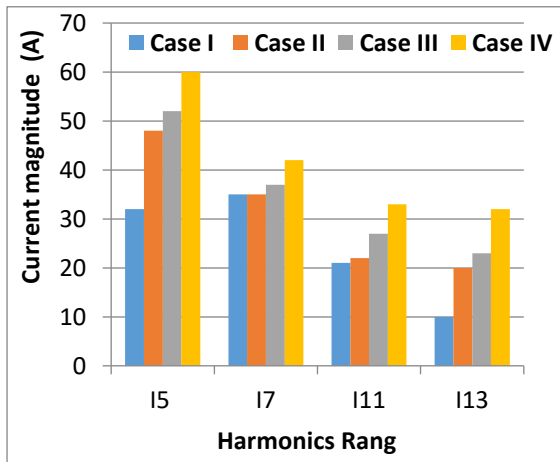


Fig. 8. Harmonics presence in a single phase

The presence harmonics current results in deformation of the total current and generate very important heating, as shown in Fig. 9(a), which will affect the magnetic field. Fig. 9(b) reveals that, the additional magnetic flux density of harmonics increases as a THD rate function at ground level.

The THD formula is presented as follows:

$$THD = \frac{\sum_{n=2}^{\infty} (I_n)^2}{I_1^2} 100\% \quad (14)$$

Where:

n is the rang of harmonic I_1 (fundamental).

The computation values of magnetic fields around 400 kV UPC without the presence of harmonics frequencies, are indicate in Table 6.

Table 6. MFs values around 400 kV UPC without the presence of harmonics

| Ground (μ T) | 1 m above the ground (μ T) |
|-------------------|---------------------------------|
| 18700 | 217 |

The obtained max values of magnetic fields computation for all cases considering harmonics effects, are depicted in Table 7.

Table 7. MFs values considering harmonics effects

| Harmonics case | at Ground (μ T) | at 1 m above the ground (μ T) |
|----------------|----------------------|------------------------------------|
| I | 2010 | 294 |
| II | 2040 | 303 |
| III | 2070 | 324 |
| IV | 2100 | 351 |

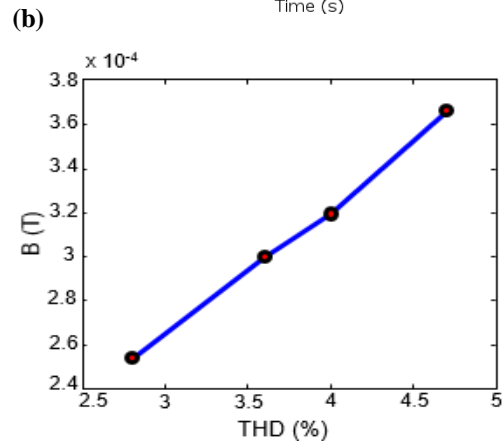
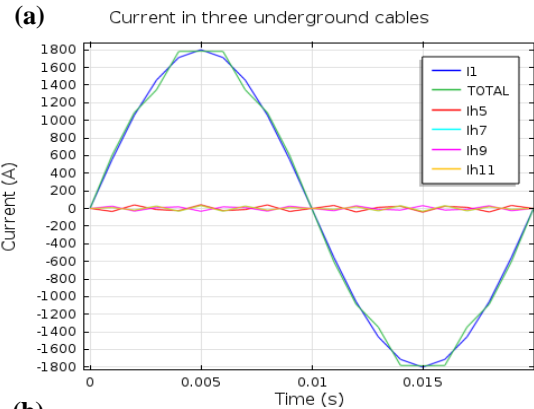


Fig. 9. Harmonics current in 400 kV UPC, (a) Current waveforms deformation caused by harmonics, (b) Maximum variation of magnetic flux density as a function of harmonics at ground level

From Table 7, we can see that the obtained values of magnetic fields are higher than the limits of the tolerable standards at ground level. Compared with exposure levels (limits) cited in Table 5, these

magnetic fields measures are above the limits at one meter (1m) above ground (294 to 351 μT). However, the harmonics circulation in underground cables leads to higher fields, mostly at ground level.

The magnetic flux density (B_x, B_y) with harmonics currents at three-phases underground cable, is illustrated in Fig. 10(a), while, the magnetic flux density with harmonics at ground level is demonstrated in Fig. 10(b).

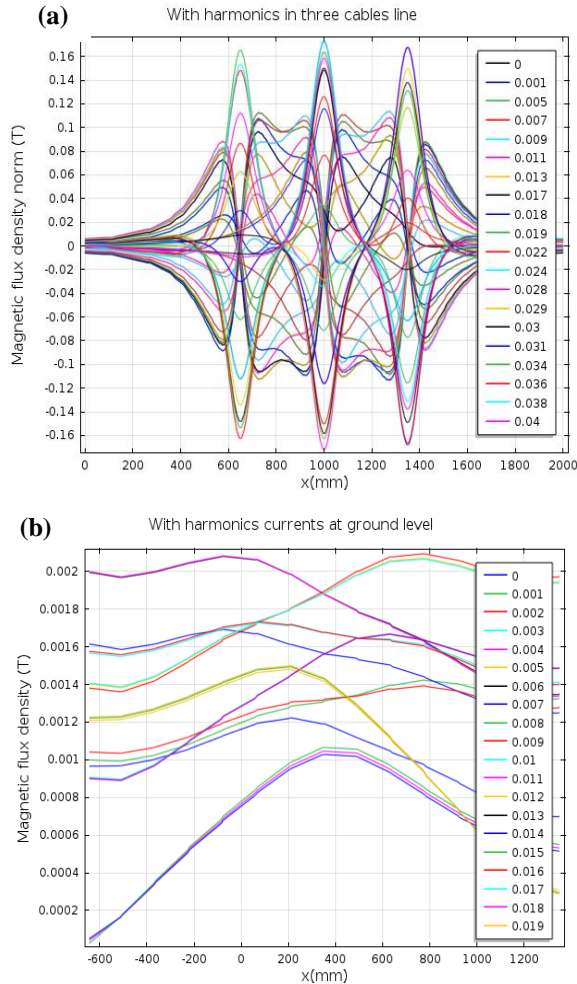


Fig. 10. The magnetic field of UPC with harmonics current, (a) magnetic flux density with harmonics at three cables, and (b) magnetic flux density with harmonics at ground level

After the comparison between Fig. 6 and Fig. 10(b), and the comparison between Fig. 7 and Fig. 10(a), we can conclude the impact and the effect of harmonics frequencies, in terms of the magnetic fields distribution, intensities, and waveform; caused by the mutual inductive effect, and additional field at different frequencies, between three cables of UPC generated by harmonics.

Fig. 11 Evaluation of the magnetic field according to the lateral distance at 1 m from the ground, Fig. 11 shows the side profiles of the calculated magnetic flux density at 1m from ground level; it appears very clearly that the magnetic flux

density magnitude (with a maximum value of 350 μT) is greater than international standard norms.

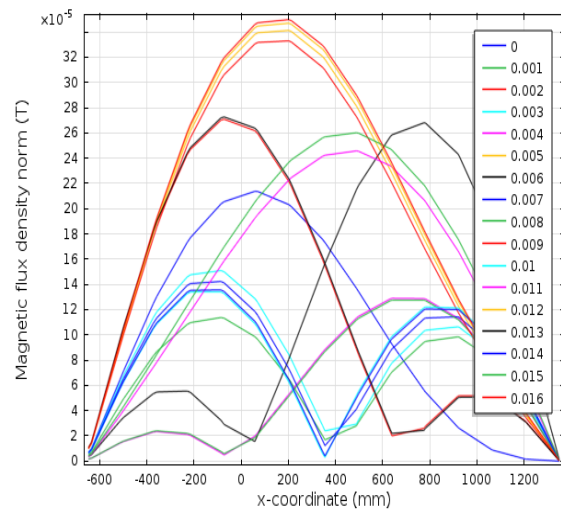


Fig. 11. MFs evaluation according to the lateral distance at 1 m from the ground

There are several solutions to reduce the effect of the harmonic current in UPCs, such as, reduction at the source of aggression, the addition of filters with power lines or in substations, distance from the depth of cables, or the addition of shielding insensitive areas ... etc.

The most common methods to attenuate the harmonics in the underground cable are:

- Passive Harmonic Filters (usually of low order (5th, 7th, 11th...)).
- Active Harmonic Filters (to cancel (or reduce) current harmonic pollution of an installation).
- Hybrid Filters (combination of passive and active), could be a good choice in certain cases.

4.3. Mitigation of magnetic field by shielding

The electric transmission lines and distribution networks generate an important low-frequency magnetic field, which greatly necessitates the development of magnetic field mitigation procedures by minimizing the intensities in the sensitive zone with the shield technique [36]–[37].

The technique is based on placing an additional mitigation system (conductive passive shield with an aluminium thickness of 4 mm), close to the source of the protected region [9], [19].

The passive compensation technique is very simple, and has a low impact ampacity and a low cost [37]–[39].

Fig. 12 reveals the conductive passive shield position near the three underground cables, and the magnetic lines are encircled between the aluminium and cables. The currents are induced in the aluminium plate due to faraday's law, which in turn;

generates a new MF that partially cancels the one from the source.

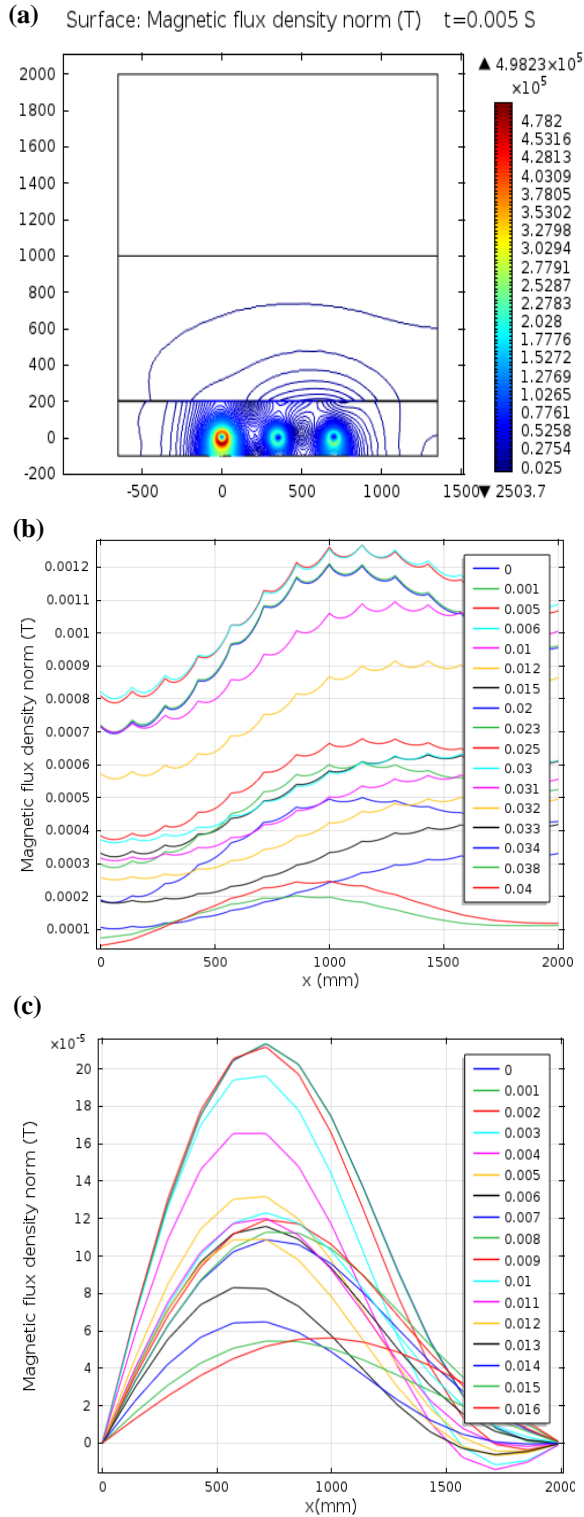


Fig. 12. Magnetic field mitigation by shielding, (a) shielding near three UPC, (b) magnetic field intensities at ground level with shield, (c) magnetic field at 1m above the ground with shield

5. CONCLUSION

In this paper, the assessment of magnetic induction emission generated by an underground

EHV cable of 400 kV, has been studied as a function of several percentages of THD of variable values in three power cable systems. A numerical simulation with time depends on the finite element method using the Comsol Multiphysics with Matlab software. The simulation results of the underground cable with two cases studies, steady states, and the presence of the harmonic with different THD, shows the magnetic field effect and concentration between three phases, intensities. However, the important harmonics circulation in underground power cables deforms the total line current and generates the additional magnetic field by increasing the amplitude and leading to higher fields mostly at ground level and one meter above the ground. The max magnetic field comparisons with international norms show excess to tolerable standards at one meter above the ground, thanks to important harmonics in the underground transmission line.

Finally, the effectiveness of shielding is proved in the magnetic field intensities and distribution attenuation through a thorough computational analysis.

In future work, we will be focused on the measure and simulation of the electromagnetic field of underground transmission lines in the presence of several faults transient or short circuits with several frequencies and magnetic field reduction by using other shielding techniques.

Author contributions: *research concept and design, H. B.; Collection and/or assembly of data, A.N.I.A., R.T., A. A.; Data analysis and interpretation, H.B., B.L., T.A.H.A.; Writing the article, H.B, A.N.I.A., T.A.H.A.; Critical revision of the article, A.N.I.A., R.T., S.S.M.G.; Final approval of the article, S.S.M.G.*

Declaration of competing interest: *The authors declare that they have no known competing financial interests or personal relationships that could have appeared to influence the work reported in this paper.*

REFERENCES

1. Dib D, Mordjaoui M. Study of the influence high-voltage power lines on environment and human health (case study: The electromagnetic pollution in Tebessa city, Algeria), *Journal of Electrical and Electronic Engineering* 2014;2(1):1-8. <http://dx.doi.org/10.11648/j.jeee.20140201.11>
2. Guo Y, Wang T, Li D, Yang H, Huang H. The review of electromagnetic pollution in high voltage power systems, *3rd International Conference on Biomedical Engineering and Informatics* 2010; 1322-1326. <http://dx.doi.org/10.1109/BMEI.2010.5639262>
3. Muratovic R, Schmutz E, Fickert L et al. Mutual inductive interference of 400 kV cable systems, *Elektrotech. Inftech. Elektrotechnik und Informationstechnik* 2017; 134: 37-45. <https://doi.org/10.1007/s00502-016-0450-6>
4. Tourab W, Babouri A, Nemamcha M. Characterization of the electromagnetic environment at the vicinity of power lines, *21st International Conference and Exhibition on Electricity Distribution CIRED11* 2011: 6-9.

5. Rezzag BI, Ayad ANEI, Larouci B, Boudjella H, Ayad A. Simulation of magnetic field pollution around in the human body in proximity of power line. The 1st International Symposium on Industrial Engineering Maintenance and Safety Oran IEMS'22, Algeria, March 5-6, 2022
6. Pawelek R, Wasiak I, Jurek M. Measurements of voltage harmonics in 400 kV transmission network, *Acta Energetica* 2014; 19(2).
<https://doi.org/10.12736/issn.2300-3022.2014205>
7. Kulkarni G, Gandhare WZ. Proximity effects of high voltage transmission lines on humans, *ACEEE International Journal on Electrical and Power Engineering* 2012; 3 (1): 28-32.
<https://doi.org/01.IJEPE.03.01.11>
8. Christou S. Thermal prognostic condition monitoring for MV cable systems, Ph.D thesis, University of Southampton, Faculty of Physical Sciences and Engineering, June 2016.
<http://eprints.soton.ac.uk/id/eprint/400225>
9. Sahin YG, Aras F. Investigation of harmonic effects on underground power cables, *International Conference on Power Engineering, Energy and Electrical Drives* 2007: 589-594.
<https://doi.org/10.1109/powereng.2007.4380123>
10. Bravo-Rodriguez JC, Del-Pino-López JC, Cruz-Romero P. A survey on optimization techniques applied to magnetic field mitigation in power systems, *Energies* 2019; 12 (7): 1332.
<https://doi.org/10.3390/en12071332>
11. European Commission (EC). 1999/519/EC Council recommendation of 12 July 1999 on the limitation of exposure of the general public to electromagnetic fields (0 Hz to 300 GHz). *Off. J. Eur. Communities* 1999; 199: 59-70.
12. Stet M. Limits of exposure to electromagnetic fields-a review of standards and regulations. *Carpathian Journal of Electrical Engineering* 2019; 13(1): 77-92.
13. Ozen NIIS, Cakir M, Carlak HF. Shielding and mitigations of the magnetic fields generated by the underground power cables," in *PIERS Proceedings* 2015: 1436-1439.
14. Souza Diogo SC et al. Experimental investigation of magnetic field shielding techniques and resulting current derating of underground power cables, *IEEE Industry Appli Society Annual Meeting* 2017: 1-7.
<http://dx.doi.org/10.1109/IAS.2017.8101877>
15. Gomes N, Almeida ME, Machado VM. Series impedance and losses of magnetic field mitigation plates for underground power cables. *IEEE Transactions on Electromagnetic Compatibility* 2018; 60 (6): 1761-1768.
<http://dx.doi.org/10.1109/TEMC.2017.2764952>
16. Canova A, Freschi F, Giaccone L, Guerrisi A. The high magnetic coupling passive loop: A steady-state and transient analysis of the thermal behavior, *Applied Thermal Engineering* 2012; 37: 154-164.
<https://doi.org/10.1016/j.applthermaleng.2011.11.010>
17. Machado VM. FEM/BEM hybrid method for magnetic field evaluation due to underground power cables, *IEEE Trans on Magnetics* 2010; 46(8): 2876-2879.
<http://dx.doi.org/10.1109/TMAG.2010.2044390>
18. Ates K, Carlak HF, Ozen S. Dosimetry analysis of the magnetic field of underground power cables and magnetic field mitigation using an electromagnetic shielding technique, *International Journal of Occupational Safety and Ergonomics* 2021: 1-11.
<https://doi.org/10.1080/10803548.2021.1918923>
19. Almeida ME, Maló Machado V, Guerreiro das Neves M. Mitigation of the magnetic field due to underground power cables using an optimized grid, *European Trans on Elect Power* 2011; 21: 180-187.
<https://doi.org/10.1002/etep.427>
20. Mohamed A, Zaini HG, Gouda OE, Ghoneim SSM. Mitigation of Magnetic Flux Density of Underground Power Cable and its Conductor Temperature Based on FEM, *IEEE Access* 2021; 9: 146592-146602.
<https://doi.org/10.1109/ACCESS.2021.3121175>
21. Kucheriava IM. Magnetic field shielding of underground power cable line by H-shaped shield, *Tekhnichna Elektrodynamika* 2020; (6): 15-20.
<https://doi.org/10.15407/techned2020.06.015>
22. Oclon P, Taler D, Cisek P, Pilarczyk M. Fem-based thermal analysis of underground power cables located in backfills made of different materials, *Strength Mater* 2015; 47: 770-780.
<https://doi.org/10.1007/s11223-015-9713-4>
23. COMSOL Multiphysics, Reference Manual 1998-2019.
24. Rachidi F. Formulation of the field-to-transmission line coupling equations in terms of magnetic excitation field, *IEEE Transactions on Electromagnetic Compatibility* 1993; 35 (3): 404-407.
<https://doi.org/10.1109/15.277316>
25. Ayad ANEI, Krika W, Boudjella H, Horch A, Benhamida F. Simulation of the electromagnetic field in the vicinity of the overhead power transmission line, *European Journal of Elect Engine* 2019; 21 (1): 49-53.
<https://doi.org/10.18280/ejee.210108>
26. Djekidel R, Bessedik SA. ASA Algorithm Combined with Current Simulation Method (CSM) for the Magnetic Induction under HV Power Lines in 3D Analysis Model, *Advanced Electromagnetics* 2020; 9 (2): 7-18. <https://doi.org/10.7716/aem.v9i2.1345>
27. Djekidel R, Bessedik SA, Mahi D, Hadjad C. Assessment of magnetic induction emission generated by an underground HV cable. *U. P. B. Sci. Bull, Series C*, 78(3), 2016, pp. 179-194.
28. Larson MG, Bengzon F. The finite element method: theory, implementation, and applications. *Engineering*. Springer Berlin Heidelberg, Berlin, Heidelberg, 2013: 71-111
<https://doi.org/10.1007/978-3-642-33287-6>
29. Wilcox DJ. Transient and harmonic induction in underground cable systems. *University of Manchester Institute of Science and Technology (UMIST)*, 1969.
30. Lilleholt LC. Technical issues related to new transmission lines in Denmark, West Coast Line from German border to Endrup and Endrup-Idomlund, technical report of Energinet 2018, Doc. 18/04246-24.
31. Swanson J. EMF Exposure Standards Applicable in Europe and Elsewhere. *Environment & Society Working Group; Connecticut Siting Council: New Britain, CT, USA*, 2006.
32. Stam R. Comparison of international policies on electromagnetic fields; power frequency and radiofrequency fields, *National Institute for Public Health and the Environment, RIVM, Netherlands* 2018.
33. ICNIRP Guidelines on Non-Ionizing Radiation Protection and others; Guidelines for limiting exposure to time-varying electric and magnetic fields (1 Hz to 100 kHz), *Health Physics* 2010; 99 (6): 818-836. <https://doi.org/10.1097/HP.0b013e3181f06c86>
34. Bailey WH, Bodemann R *et al.* Synopsis of IEEE Std C95.1™-2019 "IEEE Standard for Safety Levels With

Respect to Human Exposure to Electric, Magnetic, and Electromagnetic Fields, 0 Hz to 300 GHz, IEEE Access 2019; 7: 171346-171356.

<https://doi.org/10.1109/ACCESS.2019.2954823>.

35. Patil KD, Gandhare WZ. Threat of harmonics to underground cables, in 2012 Students Conference on Engineering and Systems, 2012: 1–6.
<https://doi.org/10.1109/SCES.2012.6199082>
36. Évo MTA, de Paula H, Lopes IJS *et al.* Study of the Influence of Underground Power Line Shielding Techniques on Its Power Capability. Journal of Control Automation and Electrical Systems 2017; 28 (4): 541-551.
<https://doi.org/10.1007/s40313-017-0319-x>
37. Del Pino-López JC, Cruz-Romero P. Magnetic field shielding of underground cable duct banks, Progress in Electromagnetics Research 2013; 138: 1-19.
<https://doi.org/10.2528/PIER13011710>
38. Ghoneim SSM, Ahmed M, Sabiha NA. Transient thermal performance of power cable ascertained using finite element analysis, Processes 2021; 9 (3): 438.
<https://doi.org/10.3390/pr9030438>
39. Djekidel R, Bessedik S. A, Spiteri P, Mahi D. Passive mitigation for magnetic coupling between HV power line and aerial pipeline using PSO algorithms optimization, Electric Power Syst Research, 2018, 165: 18-26.
<https://doi.org/10.1016/j.epsr.2018.08.014>

Received 2022-04-01

Accepted 2022-05-16

Available online 2022-05-17



Dr Houari BOUDJELLA was born in Ain Temouchent, Algeria in 1981. He graduated in Electrical Engineering from Djillali Liabes University of Sidi Bel Abbes, Algeria in 2004 as electrical engineer, received the Magister degree in Electrical Engineering from the same University in 2008, and the Ph.D. (Engineering)

from the University of Sciences and Technology Mohammed Boudiaf USTO -MB, Oran Algeria in 2021. Presently, he is a lecturer in Electrical Engineering, and he is serving as assistant Professor in the Department of Electrical Engineering, Kasdi Merbah University, Ouargla, Algeria since 2013. Member at sustainable development laboratory of electrical energy (LDDEE), USTO-MB, Oran, Algeria. His research interest includes power system operation and planning, soft and evolutionary computing, intelligent methods for power system optimization and smart grid planning, FACTS devices.



Dr Ahmed Nour El Islam AYAD is a lecturer in Electrical Engineering, was born in Sidi Bel Abbes Algeria 1985. He received his Magister and Ph.D in 2011, and 2017 respectively in electrical engineering, from Djilali Liabes University, Algeria. From 2014 to present, he was an assistant professor at Kasdi Merbah

University, Ouargla, Algeria. His major fields of interest

are eddy current and magnetic separator process, EMC, electromagnetic environment pollution, electric cable



Dr Tahar ROUIBAH was born in Jijel, Algeria, on Jun 19, 1978. He received the State Engineer in electrical engineering Option: Electrical Networks from the University of Jijel, Algeria, in 2002, Magister in electrical engineering from the University of Constantine, Algeria, in 2005 and Ph.D in EE from the University of Setif, Algeria, in 2015. His research interests include lightning protection systems, earthing design, and wind turbine generators.



Dr Benyekhlef LAROUCI is a PhD in Electrical Engineering, was born in 1985 in Mascara, Algeria. He is currently works at Kasdi Merbah University Ouargla, Algeria. He received a Ph.D degree and Magister in Electricals engineering from the University of Science and technology of Oran, Algeria in 2018. He received a Diploma Engineer in Electrotechnics from the University of Mascara in 2007. His research activities are in the power system optimization, including economic dispatch, the heuristic optimization techniques and include the control of large power systems, Facts devices and the unified power flow controller.



Pr Sherif S. M. GHONEIM received the B.Sc. and M.Sc. degrees from the Faculty of Engineering at Shoubra, Zagazig University, Egypt, in 1994 and 2000, respectively, and the Ph.D. degree in electrical power and machines from the Faculty of Engineering, Cairo University, in 2008. Since 1996, he has been teaching at the Faculty of Industrial Education, Suez Canal University, Egypt. From 2005 to 2007, he was a Guest Researcher with the Institute of Energy Transport and Storage (ETS), University of Duisburg-Essen, Germany. After that, he joined the Department of Electrical Engineering, Faculty of Engineering, Taif University, as an Associate Professor. His research interests include grounding systems, dissolved gas analysis, breakdown in SF6 gas, and AI technique applications.